Accepted Manuscript

Analysis of the Failure of Cracked Biscuits

Evangelina Garcia-Armenta, Gustavo Gutierrez, Saurabh Anand, Kevin Cronin

PII:	S0260-8774(16)30376-4
DOI:	10.1016/j.jfoodeng.2016.10.015
Reference:	JFOE 8692
To appear in:	*Journal of Food Engineering*
Received Date:	09 October 2015
Revised Date:	12 August 2016
Accepted Date:	12 October 2016

- Effect of cracks on biscuit strength was explored.
- Failure by overstressing was compared to failure by crack propagation.
- Tensile strength and fracture toughness were measured experimentally.
- Experimental results were confirmed by theoretical analysis.

Analysis of the Failure of Cracked Biscuits

Evangelina Garcia-Armenta[1], Gustavo Gutierrez[1], Saurabh Anand[2], Kevin Cronin[2*]

[1]Departamento de Graduados e Investigación en Alimentos. Escuela Nacional de Ciencias Biológicas. Instituto Politécnico Nacional. Carpio y Plan de Ayala S/N. Col. Santo Tomás, C.P. 11340. D.F. Mexico.

[2]Department of Process & Chemical Engineering
University College Cork, Cork, Ireland
*Corresponding author k.cronin@ucc.ie

ABSTRACT

Cracks or checks in biscuits weaken the material and cause the product to break at low load levels that are perceived as injurious to product quality. In this work, the structural response of circular digestive biscuits, with diameter 72 mm and thickness 7.2 mm, simply supported around the circumference and loaded by a central concentrated force was investigated by experiment and theory. Tests were conducted to quantify the distribution in breakage strength for structurally sound biscuits, biscuits with natural checks and biscuits with a single known part-through crack. For sound biscuits the breakage force is Normally distributed with a mean of 12.5 N and standard deviation of 1.2 N. For biscuits with checks, the corresponding statistics are 9.6 N ± 2.62 N respectively. The presence of a crack weakens the biscuit and strength, as measured by breakage force falls almost linearly with crack length and crack depth. The orientation of the crack, whether radial or tangential, and its location (i.e. position of the crack mid-point on the biscuit surface) are also important. Deep, radial, cracks located close to the biscuit centre can reduce the strength by up to 50 %. Two separate failure criteria were examined for sound and cracked biscuits respectively. The results from these tests were in good accord with theory. For a biscuit without defects, breakage occurred when maximum biscuit stress reached or exceeded the failure stress of 420 kPa. For a biscuit with cracks, breakage occurred as above or alternatively when its critical stress intensity factor of 18 kPam$^{0.5}$ was reached.

Keywords: Biscuits, Fracture, Cracks, Stress Intensity Factor

NOTATION

a	Crack half length	m
b	Biscuit sample width	m
g_1	Crack depth to biscuit thickness parameter	-
g_2	Crack length to biscuit thickness parameter	-
K_I	Stress intensity factor	kPa $m^{0.5}$
K_{IC}	Critical stress intensity factor	kPa $m^{0.5}$
L	Support span length	m
P	Applied force	N
R	Biscuit radius	m
r	Radial distance	m
r_c	Crack radial location (mid-point)	m
r_0	Radius of applied load	m
r_0’	Equivalent loading radius	m
t	Biscuit thickness	m
w	Crack depth	m
x	Linear distance	m
α	Crack angular orientation	rad
σ	Stress	kPa
ν	Poisson’s ratio	-
θ	Angle	rad

1. INTRODUCTION

Biscuits are one of the most consumed snack-type products across the world by all levels of society (Okpala and Okoli, 2013). Their popularity is mainly due to their sweet taste, ready-to-eat nature, affordable cost, nutritional value and long shelf life (Sudha et al., 2007; Vujic et al., 2014). One of the most important quality features of biscuits is texture (Mamat and Hill, 2012). Texture depends on many factors including the structure of the biscuit and methods of manufacturing and handling during the process. Texture is the mechanical strength of the biscuit quantified by the load required to produce failure by fracture. From a physical basis, this load can be taken as equivalent to the critical stress level at which an existing flaw propagates through the material and leads to breakage of the biscuit (Kim et al., 2012). Hence the fracture properties of the biscuit must be understood. Fracture properties relate the loading on a biscuit to its structural response and particularly to the propagation of cracks leading to failure. For biscuits this is also related to the phenomenon of checking.

For almost a century, biscuit manufacturers have sought to avoid 'checking' This can be defined as the appearance of small hairline cracks in biscuits after baking that affects fragility and product degradation (hence checks are naturally occurring cracks resulting from the baking process). This phenomenon of crack formation can occur during the industrial cooling of the biscuits as a consequence of the stresses generated by dimensional changes associated with equilibration of moisture due to moisture gradients within the freshly baked biscuit (Manley, 2000).These cracks extend from the centre towards the periphery, making the whole structure weak and giving the possibility for the biscuit to break spontaneously (Dunn & Bailey 1928). The drying process in the last zones of the baking oven inevitably causes the central and thicker parts of the biscuit to have slightly more moisture than the outer zones. During subsequent cooling and storage, moisture diffuses from regions of high moisture content (centre) to areas with less moisture (edges), which also take up moisture from the surrounding environment. This moisture migration leads to expansion towards the edge of the biscuit and contraction at the centre, causing stresses to build up in the biscuit. Depending on the physical properties of the biscuit structure as it cools, cracks may develop when these stresses exceed a critical value Manley, (1983).

In addition to the possible presence of checks or cracks, it should be understood that baked biscuits contain a very large number of pores ranging in size from 10 μm up to 300 μm, (Pareyt et al., 2009). The pores are formed as a result of water vapour production and expansion during the baking process. Morphology of these pores can vary from rounded to very angular. Long narrow, notched pores can act as sites of stress concentration and hence as crack initiation points while large rounded pores in the structure offer the possibility of arresting the propagation of cracks. Thus the microstructure of the biscuit has an effect on its physical and sensory properties (Frisullo et al., 2010). The value and functionality of most of the brittle food products rely on their cellular foam structure that is strongly linked to texture (Lim and Barigou, 2004). The complex non-uniformity in the internal structure of the biscuit means the process of crack propagation in such materials, compared to homogenous ones, possesses additional features due to their randomness. The random distribution of pores in location, size and shape makes the fracture of porous materials difficult to predict. Contradictory results are often reported in the fracture of porous materials; strengthening and weakening. No simple relationship is possible as the fracture performance depends on the distribution in pore size, shape and location (Legullion & Piat, 2007). These two effects of non-uniformity of the internal porous structure and randomness associated with the potential presence of checks causes the well-known scatter in strength and fracture parameters.

Superimposed on the phenomenon of fracture is the fact that the presence of pores also influences the effective elastic constants and a random redistribution in the nominal stress, (Ramakrishnan & Arunachalam, 1990). Thus many researchers who have examined brittle, porous foods have considered them to act as a homogeneous, elastic solid using nominal values for the mechanical properties of the homogenised sections (Rojo & Vincent, 2008). The other approach involves very detailed morphological structural modelling with finite element analysis (Guessasma et al., 2011). Most previous work reported in the literature has involved the measurement of the strength and fracture properties of biscuits using the standard three point bending tests, (Saleem, 2005). The aim of this work was to examine the dispersion in breakage force and breakage pattern for uncracked and cracked biscuits in an axisymmetric bending load test. In addition, the effect of crack geometry on breakage force was explored and experimental tests used to identify an appropriate theoretical model of biscuit failure.

2. THEORY

2.1 Biscuit Loading

Each biscuit was loaded by applying a point force at its centre while its circumference rested on a smooth circular ring as illustrated in figure 1. This method is not representative of the actual loading of biscuits during manufacture, storage and transportation; however it provided a rational basis to quantify the bending strength of circular biscuits. Based on this arrangement, each biscuit was considered a thin, flat circular plate, simply supported around its perimeter and loaded by a concentrated force, P applied at its centre. The lower surface of the biscuit is in a state of tension due to the induced two-dimensional bending response of the biscuit with two orthogonal, normal, tensile stresses in the radial and circumferential directions respectively. These can be predicted as follows (Benham et al., 1996):

$$\sigma_r = \frac{3P(1+\upsilon)}{2\pi t^2}\ln\left(\frac{R}{r}\right) \qquad \sigma_\theta = \frac{3P(1+\upsilon)}{2\pi t^2}\left[\ln\left(\frac{R}{r}\right)+\frac{1-\upsilon}{1+\upsilon}\right] \quad \mathit{for} \quad r \neq 0 \qquad (1)$$

The circumferential (tangential) stress acts in the perpendicular direction to any radial line while the radial stress is perpendicular to a circumferential curve. Both stresses decrease rapidly with radial distance and are considerably lower at the edge than at the centre of the biscuit. The circumferential stress is always the larger of the two and the fractional difference between σ_θ and σ_r increases when moving from the centre of the biscuit to the perimeter. The predictions for stress in equation 1 exhibits a discontinuity at the origin (r = 0) and tend to infinite magnitudes at that position. This arises because the load is considered to act at a point whereas in reality the load is applied over a small central area of radius, r_0. It has been shown that the maximum stresses in the plate (at either surface) are limited to the following levels (Young, 2001)

$$\sigma_r = \frac{3P(1+\upsilon)}{2\pi t^2}\ln\left(\frac{R}{r_0'}\right) \qquad \sigma_\theta = \frac{3P(1+\upsilon)}{2\pi t^2}\left[\ln\left(\frac{R}{r_0'}\right)+\frac{1}{1+\upsilon}\right] \qquad (2)$$

where r_0’ is the equivalent loading radius defined as

$$r_0' = \sqrt{1.6r_0^2 + t^2} - 0.675t \qquad (3)$$

Hence in the central region of the biscuit (0 < r < r_0’), if the predicted values of σ_θ and σ_r from equation 1 are in excess of those estimated using equation 2, they are replaced by the latter values. Figure 2 illustrates the variation of tangential and radial stress with radial distance from the biscuit centre to the edge using data representative for the study.

The stress equations require knowledge of the Poisson’s Ratio for these biscuits. Kim et al., (2012), suggested a value of 0.2 as appropriate for this material. This is an estimate but a sensitivity analysis revealed that the level of uncertainty in the correct magnitude of Poisson’s Ratio does not meaningfully affect the predictions of stress; the fractional variation in resultant stress is considerably lower (more than 50 %) than the fractional uncertainty in Poisson's Ratio. It should also be noted that material behaviour was considered to be isotropic and so only a single value for the Poisson's Ratio was needed.

2.2 Maximum Tensile Perpendicular Stress

For the subsequent fracture mechanics analysis, the maximum tensile stress acting perpendicular to any line segment, $\sigma_{\perp}$ of length 2a on the biscuit lower surface must be estimated. For a line (crack) acting in the radial direction, this stress will be the tangential stress at the point in the crack closest to the biscuit centre, as illustrated in figure 3a. If the line passes through the centre, $\sigma_{\perp}$ will coincide with the limiting stress of equation 2. For a line acting in the tangential direction, the situation is more complex. At the mid-point of the line, the perpendicular stress is the radial stress at that location. At any other point along the line, the perpendicular stress is a function of both the radial and tangential stress at the location in question. At any distance, x, ($x < r_c$) along the line that subtends an angle θ as shown in figure 3b, the tensile perpendicular stress will be (Benham et al., 1996):

$$\sigma_{\perp} = \sigma_{\theta}\frac{1+\cos 2\theta}{2} + \sigma_{r}\frac{1-\cos 2\theta}{2} \qquad (4)$$

Using the trigonometric relationships $r = \sqrt{r_c^2 + x^2}$ $\qquad \tan\theta = \frac{r_c}{x}$ $\qquad$ (5)

The perpendicular stress along the line can be expressed as

$$\sigma_{\perp} = \frac{3P(1+\upsilon)}{2\pi t^2}\left\{\ln R + \frac{1-\upsilon}{1+\upsilon}\frac{x^2}{r_c^2 + x^2} - \ln\left(r_c^2 + x^2\right)^{\frac{1}{2}}\right\} \quad 0 \le x \le a \qquad (6)$$

Equation 6 gives the tensile perpendicular stress at any point along a tangential line at a distance, x from the midpoint of the crack. Figure 3c illustrates how $\sigma_{\perp}$ varies with distance along the line. The perpendicular stress rises from a value equal to the radial stress at the midpoint, reaches a maximum value at some distance along the line and then falls off. For a line segment defined by an angle other than 0 (radial line) and 90° (tangential line), the

ACCEPTED MANUSCRIPT

perpendicular stress has a more complicated relationship with distance along the line and was evaluated numerically in this paper.

2.3 Biscuit Failure Criteria

To predict failure, the stress state in the biscuit must be combined with a valid failure criterion. A biscuit is linearly elastic and breaks suddenly with minimal plastic deformation indicating that it can be considered as a brittle material once its temperature is below the glass transition temperature for the product. For the digestive-type biscuits of this study, the glass transition temperature, T_g is well above room temperature (T_g = 62.8°C) (Kawai et al., 2014). The following cases were considered; 1] the biscuit contained no cracks or defects and 2] cracks were present.

For the former, the appropriate failure theory is the maximum principal stress theory and for the loading situation described above, this corresponds to the maximum circumferential stress at the centre of the biscuit (predicted by equation 2) exceeding the tensile strength of the biscuit at failure, σ_f (Haghighi and Segerling, 1988).

$$\sigma_{\max} \geq \sigma_f \quad \Rightarrow \quad failure \qquad (7)$$

In other words the biscuit is predicted to fail when the applied load, P is sufficient to ensure the tangential stress, σ_θ at the biscuit centre reaches a maximum value that equals the material strength of the biscuit, σ_f.

If the biscuit contained cracks, each crack was considered to have the geometry of a straight, part-through crack (crack depth being limited to less than half biscuit thickness) of finite length (crack half-length being limited to less than biscuit radius). A crack is defined by the following four geometric properties; length 2a, depth w, radial distance from biscuit centre to the midpoint of the crack, r_c and angle subtended at the mid-point between a radial line and the crack line. The geometry is illustrated in figure 4. A crack or check will propagate if a sufficiently large in-plane tensile stress is applied normal to the crack plane (assuming mode 1 fracture i.e. the crack opening mode by tension). Specifically if the stress intensity factor, K_I exceeds the critical stress intensity factor, K_{IC} for the crack, then failure by fracture is predicted, (Van Vliet, 2014).

$$K_I \geq K_{IC} \quad \Rightarrow \quad failure \qquad (8)$$

For this paper, the stress intensity factor proposed by Rice & Levy (1972) for a part-through surface crack of finite length in an elastic plate under a bending load was selected as the closest analysis to our case. K_I is shown to be a function of plate (biscuit) thickness, the magnitude of the perpendicular stress, the ratio of crack depth to plate (biscuit) thickness and the ratio of crack length to plate thickness:

$$K_I = g_1\, g_2\, \sigma_{\perp} \sqrt{t} \qquad (9)$$

For the analysis it is assumed that the presence of a crack does not significantly change the overall stress distribution and only the local distribution in the crack region. Moreover as biscuit thickness to biscuit diameter ratio is equal to 0.1, the biscuit is treated as a thin cylinder subject to plane stress. The approximations made in discounting the 3D nature of stress in the structure were discussed more fully by Rice & Levy (1972) and by Yang & Shiva (2011). The dimensionless factors g_1 and g_2 are derived from the semi-analytical analysis presented in the work of Rice & Levy (1972). Specifically g_1 is solely a function of the ratio of crack depth to plate thickness while g_2 is additionally a function of crack length to plate thickness ratio. The following modified 4th order polynomial was used to express the g_1 parameter in terms of relative crack depth

$$g_1 = \sqrt{\frac{w}{t}}\left(1.99 - 2.47\frac{w}{t} + 12.97\left(\frac{w}{t}\right)^2 - 23.17\left(\frac{w}{t}\right)^3 + 24.80\left(\frac{w}{t}\right)^4\right) \qquad (10)$$

while the g_2 parameter can be represented by a fitted empirical equation (for the range of data of interest to this paper) extracted from Rice & Levy (1972) of the form

$$g_2 = c_1 \ln(2a/t) + c_2 \qquad (11)$$

where the constants c_1 and c_2 depend on the relative crack depth (w/t). Table 1 gives the magnitudes of these constants for a number of relative crack depth ratios. The g_1 parameter increases monotonically from 0 to close to 1.5 as the ratio of crack depth to biscuit thickness increases from 0 (very shallow crack) to 0.5 (deep crack) quantifying the influence of crack depth on the stress intensity factor. For shallow cracks, the g_2 parameter and hence stress intensity factor is relatively insensitive to crack length but for deeper cracks, the stress intensity factor will increase significantly with crack length. Overall, the longer and deeper the crack, the larger is the stress intensity factor and the greater the likelihood of biscuit breakage.

2.4 Determination of Critical Crack Size

The presence of cracks weakens the biscuit by reducing the required breakage force. Critical crack size is the crack dimension at which the biscuit will fail by fracture rather than overloading. The seriousness of a crack depends on its size (depth and length) and its radial location and angular orientation on the biscuit surface. Qualitatively from the stress intensity factor approach, the deeper the crack, the longer the crack, the more central the crack and the more radial in inclination, the lower is the required breakage force. Also while all these factors affect biscuit integrity, crack depth is more influential than crack length in determining the response and crack radial location is more significant than crack orientation. However because of the complexity of the stress intensity factor model and the non-uniformity of the stress distribution in the biscuit, it is not possible to produce a simple analytical formula for critical size for a general crack.

For the restricted case of a very shallow crack that is long relative to biscuit thickness, an analytical approach can be conducted. In this situation, for the selected SIF (Stress Intensity Factor) of equation 9, the g_1 parameter is approximately equal to $2\sqrt{\frac{w}{t}}$ while the g_2 parameter has a value of almost 1. Hence the SIF is solely dependent on crack depth, w and is given as

$$K_I = 2\sigma_{\perp}\sqrt{w} \qquad (12)$$

Also if this crack passes through the central region of the biscuit, where both the tangential and radial stress are limited and furthermore in this region the perpendicular stress is almost equal to the average of the radial and tangential stresses and can be approximated as

$$\sigma_{\perp} = \frac{3P(1+\upsilon)}{2\pi t^2}\left[\ln\left(\frac{R}{r_0^{'}}\right) + \frac{1}{2(1+\upsilon)}\right] \qquad (13)$$

Thus the criterion for biscuit failure by fracture will be

$$\frac{3P(1+\upsilon)}{2\pi t^2}\left[\ln\left(\frac{R}{r_0^{'}}\right) + \frac{1}{2(1+\upsilon)}\right] 2\sqrt{w} = K_{IC} \qquad (14)$$

While the criterion for failure by overloading is when the maximum stress (equal to the limited tangential stress) equals the failure stress

$$\frac{3P(1+\upsilon)}{2\pi t^2}\left[\ln\left(\frac{R}{r_0^{'}}\right) + \frac{1}{1+\upsilon}\right] = \sigma_f \qquad (15)$$

By combining equations 14 and 15, it was possible to estimate the necessary crack depth that will cause failure by fracture rather than overloading to occur

$$w \geq \left\{ \frac{\left[\ln\left(\frac{R}{r_0^{'}}\right) + \frac{1}{(1+\upsilon)}\right] K_{IC}}{\left[\ln\left(\frac{R}{r_0^{'}}\right) + \frac{1}{2(1+\upsilon)}\right] 2\sigma_f} \right\}^2 \qquad (16)$$

Thus when the magnitude of crack depth exceeds the value predicted by the expression in equation 16, failure by fracture is predicted to occur. This formula is applicable to a long, shallow crack that passes through the central zone (where the load is applied) of any angular orientation.

3. MATERIALS & METHODS

3.1 Materials

The biscuits used in this study were obtained from a commercial manufacturer (own brand supermarket variety) and were of the digestive type. Typical composition was 22.3 % fat, 18.8 % sugars, 3.5 % fibre, 6.7 % protein and 1 % salt. The average moisture content was measured by the oven dry test and found to be 1.55 ± 0.19 % wet basis. The average porosity was measured using the Kawas and Moreira (2001) approach of using values of the bulk density and the solid density of the biscuit. Bulk density was obtained using a modified Archimedean method replacing the displacement of a fluid for the displacement of 1 mm solid-glass spheres (Consolmagno and Britt, 1998); solid density was measured by placing a fragment of the biscuit in a compressed helium gas multivolume pycnometer (Micromeritics, Model 1305, USA). These tests were performed in five replicates. Each biscuit tested had its diameter and thickness recorded in which the average of three readings were taken with a Vernier digital caliper (Mitutoyo, model 500-151-30, Japan).

The biscuits were divided into three classes. The first included all biscuits containing no visible checks these being most of the biscuits. The second class consisted of those biscuits that had visible checking. The checks were all superficial i.e. very shallow on the surface of the biscuit. There were many checks (ten or more) on each biscuit. Each path was random in orientation and jagged as opposed to straight. These checks were present on all locations of the biscuit surface i.e. close to the edge and near the centre. Typical lengths ranged from 10 mm to 30 mm. Finally tests were conducted on biscuits that had pre-defined cracks placed in them to explore the effect of cracks on biscuit structural response. The cracks were made with a thin blade having a thickness of 2 mm. Most of the cracks were either radial or tangential in orientation though a small number of tests were done with other crack angles. In total, 18 different crack types (labelled A to R) were investigated with 15 replicates used for each type. Table 2 lists the geometrical parameters (orientation, length, mid-point location and depth) for each crack type. Additionally the geometries of each crack type are graphically displayed in figure 5 where the length and orientation of the crack and the distance from its midpoint to the biscuit centre (when non-zero) are indicated by the arrowed line.

3.2 Three Point Bending Tests

The standard three point bending tests was first carried out to obtain values for the material properties of failure stress, σ_f and the critical stress intensity factor, K_{IC}. Prismatic specimens were cut from the biscuits with rectangular sides of 60 mm by 20 mm and 7.2 mm thick. These were supported on parallel bars, 40 mm apart and loaded by a third bar (line load) equi-distant between the two support bars. The tests were performed on a Texture Analyser (TA.HDplus, Stable Micro Systems, UK). In total, 20 samples were tested. Force versus deflection was recorded until the biscuit specimens broke. The failure stress can be quantified from

$$\sigma_f = \frac{3PL}{2bt^2} \qquad (17)$$

where P is the measured load at failure, b is the cross section dimension of the beam (20 mm), t the beam depth (7.2 mm) and L the bar spacing or beam span (40 mm).

Experiments were also conducted with these specimens to estimate the fracture toughness. A total of five samples were used. The sample was re-orientated so that equivalent beam depth, t was 20 mm and beam cross section dimension, b 7.2 mm. A notch of 10mm depth and running through the thickness of the sample was made at the bottom face. A line load was applied at its centre of the span and for this work the supports spacings, L were 45 mm apart. Fracture toughness or critical stress intensity factor, K_{IC} was quantified in accordance (ASTM, 2008)

$$K_{IC} = \frac{PL}{bt^{\frac{3}{2}}} f\left(\frac{w}{t}\right) \qquad (18)$$

with $$f\left(\frac{w}{t}\right) = \left[1.9 - \frac{w}{t}\left(1-\frac{w}{t}\right)\left(2.15 - 3.93\frac{w}{t} + 2.7\left(\frac{w}{t}\right)^2\right)\right] \frac{3\sqrt{\frac{w}{t}}}{2\left(1+2\frac{w}{t}\right)\left(1-\frac{w}{t}\right)^{1.5}} \qquad (19)$$

Owing to limitations of possible sample dimensions, the adopted test procedure was not in strict accord with ASTM specification for the measurement of fracture toughness (as the beam depth of 20 mm was too low). Hence the estimated levels of K_{IC} can only be regarded as indicative.

3.3 Axi-Bending Tests

Regarding the axi-symmetric bending tests, three sets of loading tests were performed on the texture analyser for biscuits with no visible checks, for biscuits with naturally occurring checks and lastly for biscuits with pre-defined checks. In each case, the biscuit was supported by resting on a thin steel ring with a circumference of 34 mm radius. The loading indenter with a tip radius, r_0 of 3 mm was applied at the centre of the biscuit. From equation 3 (using a biscuit thickness of 7.2 mm) the equivalent loading radius r'_0 was 3.28 mm which limits the maximum stress at the biscuit inside this zone. Loading speed was 1 mm/s. Force versus deflection was measured up to the point of breakage. The broken biscuit was photographed after fracture and the crack shape and fragment distribution analysed. For some tests, high speed photography was employed to investigate the dynamic progression of the crack at the point of breakage.

4. RESULTS & DISCUSSION

4.1 Physical & Mechanical Properties of Biscuits

The variation in diameter and thickness between biscuits was found to be described by the Normal distribution. Mean and standard deviation for diameter were 71.7 ± 0.9 mm respectively and for thickness 7.2 ± 0.3 mm, respectively. Bulk density was 463.18 kg/m^3, solid density 1401.4 kg/m^3 and hence porosity was estimated to be 67 % (0.67). From the three-point bending tests, the tensile strength of the biscuits had a mean value of 420 kPa and standard deviation of 31 kPa, (420 ± 31). These were in good agreement with values reported in the literature for semi-sweet biscuits (Kim et al., 2012), Ahmad (2001) and Saleem (2005). The average K_{IC} value obtained from notched bending test was 18 kPam$^{0.5}$ with a standard deviation of 3.0 kPam$^{0.5}$ (18.0 ± 3.0). While this value can only be regarded as an estimate, it does lie at the lower end in the range of values reported by Kim et al., (2012). The coefficient of variation is considerably larger for the fracture toughness than for tensile strength indicating a much higher level of natural dispersion for the former quantity. While this may reflect experimental sample size effects, it could also indicate that fracture toughness is more sensitive to the random and heterogeneous structure of the biscuit than tensile strength.

4.2 Failure of Un-Checked Biscuits

In total over 160 biscuits with no visible defects were loaded under axisymmetric bending until failure occurred. The distribution in maximum breakage force is shown in frequency histogram form in figure 6. The average magnitude of the breakage force was 12.5 N, the standard deviation was 1.2 N (12.5 ± 1.2) and it ranged from a minimum of 9.7 N to a maximum value of 15.3 N. The distribution in failure force can be represented by the Normal distribution. Video analysis indicated that the cracks tended to start where the load was applied and propagate out along the radial direction to the edge. All the biscuits fractured in tension along a lower line at the lower surface where maximum stresses are predicted. Biscuit breakage patterns conformed to three basic types; two radial cracks (either collinear or non-collinear); three radial cracks and four radial cracks. Each type is illustrated in figure 7. The majority of the biscuits, 67 % failed with the formation of three cracks while 26 % produced two cracks with only 7 % giving four radial cracks. Higher breakage forces are associated with a larger number of fracture planes but not at a statistically significant level.

The validity of the proposed failure criterion for un-checked or sound biscuits given by equation 7 was then checked. A biscuit will fail when the predicted maximum stress (the limited circumferential stress predicted using equation (2) exceeds the tensile strength value reported in section 4.1 above. The issue is complicated because the measured value of tensile strength is statistically distributed and the distribution in biscuit thickness (and any other parameters in equation 2) affects the predicted stress value. Hence the validity of equation 7 must be tested statistically. The experimentally measured tensile strength (from the 3 point bending test) is 420 ± 31 kPa. The predicted failure stress (obtained from equation 2 using the measured failure force) is 438 ± 42.1 kPa. While the predicted failure stress value is larger than the experimentally measured failure stress, the difference between them is not statistically significant (at the 5 % confidence level using the t statistic) demonstrating that the criterion of equation 7 is valid.

4.3 Failure of Checked Biscuits

Breakage force for biscuits with the presence of checking was also recorded. In total 50 biscuits exhibiting checking were loaded and broken. Figure 8 illustrates such checked biscuits. Mean breakage force for the biscuits was 9.6 N and the standard deviation 2.62 N (9.6 ± 2.62) compared to (12.5 ± 1.2) N respectively for unchecked biscuits. The average breakage force for checked biscuits is 23 % lower than for the unchecked product demonstrating the significant influence of checking on biscuit integrity. Moreover the standard deviation in breakage force for checked biscuits is over twice as large as for unchecked indicating much greater dispersion in strength which is also an adverse quality feature. Caution is required in interpreting these results because of the very heterogeneous nature of the checks that were present and lack of accurate characterisation of their precise geometry. Nonetheless it is clear that when checking occurs, it has a major impact on biscuit strength and resistance to breakage. No theoretical analysis was carried out into the failure of these biscuits. Each biscuit tended to have more than one check on its surface and each check had a complex, tortuous path precluding any analytical application of fracture mechanics theory. However these results clearly demonstrate that defects such as checks significantly affect biscuit strength and hence quality and underlie the importance of investigations in this area.

4.4 Failure of Cracked Biscuits (Experimental)

In total, 18 different crack types were investigated. For each type, both the mean and standard deviation in breakage force was quantified. In addition, the reason for failure (overloading or crack propagation) was noted. The presence of a crack in the biscuit does not automatically mean that failure is as a result of crack propagation when the load is applied; if the maximum stress in the biscuit exceeds the failure stress before the local stress intensity factor exceeds the critical stress intensity factor, then failure is due to overloading. There are two aspects to breakage that indicate the failure mode; the location of the fracture plane and the magnitude of the failure force. If the fracture plane initiates at the biscuit centre (where stress is maximum), this is indicative of failure due to overloading as is the case for an uncracked biscuit. If the fracture plane initiates at the defined crack, then this can be taken to be failure resulting from crack propagation. Also an uncracked biscuit requires a breakage force of 12.5 N. Breakage forces in this region are indicative of failure by overloading while as the measured breakage force falls away from these levels, failure by crack propagation is more likely. Owing to the intrinsic variability in the breakage force (which ranges from 10 N up to 15 N), this parameter alone is not a definitive indicator. Table 3 summarises the experimental results for the cracks giving the crack type, breakage force statistics and failure mode. At the top of the table the corresponding results for a biscuit without cracks are shown for comparison.

As shown in table 3, crack types A, B, C, D are all radial cracks, with a midpoint at the biscuit centre and 1 mm deep. The breakage force fell consistently from 11.76 N (crack A) to 8.27 N (crack D) as crack length increased from 5 mm to 70 mm respectively. Crack types E, F, G, H differed from the above by just being 2 mm deep. Breakage force followed the same pattern as above, falling from 9.76 N (crack E) to 6.5 N (crack H) though in all cases was lower reflecting the fact that the cracks are deeper and so the biscuits failed more easily. For these eight crack types, failure was by crack propagation. Figure 9 plots breakage force versus crack length for the two crack depths that were analysed. There is a definite, almost linear, relationship between breakage force and the length of the crack and a clear relationship between crack depth and breakage force. Long, deep cracks can reduce the strength of a biscuit by up to 50 % compared to an uncracked biscuit.

Cracks I, J and K are also radial though all having a midpoint at 15 mm from the biscuit centre so the local stress at the crack will be lower than for the previous eight cracks. Crack type I was short (5 mm in length) and the biscuit did not fail by crack propagation but by overloading with a high breakage force of 11.82 N. The biscuits with crack types J and K failed by crack propagation with the breakage force of close to 9 N. Breakage force is generally higher for these three crack types than the previous radial cracks because they are less heavily stressed being away from the biscuit centre. Finally crack type L is also radial though short in length (5 mm), relatively shallow (1 mm) and quite removed from the biscuit centre with its midpoint at a radial distance of 27.5 mm. Thus the stress at it is relatively low and hence the biscuit failed by overloading with a high breakage force of 9.92 N.

Crack types M, N, O and P are all tangential in orientation. For tangential cracks, radial stress will be the critical perpendicular stress which is lower than tangential stress. These cracks are all 1 mm deep but the length and mid-point radial location vary. Crack types M, N and O are at a considerable distance from the biscuit centre where the maximum stress acting on the crack is low and so the biscuits all failed by overloading with the breakage force always exceeding 9 N. Only crack type P which was 5 mm from the centre caused the biscuit to fail by crack propagation and had the lowest breakage force of the four types of tangential crack. Finally the table gives the data for two cracks types (types Q and R) whose midpoint orientations are defined by the angles of 30°and 60° respectively. For these cracks it was not possible to definitively state the failure mechanism although the crack pattern was more indicative of failure by overload. For all the crack types explored, the standard deviation in breakage force was of the same order of magnitude as that for an uncracked biscuit (1.2 N). Hence the presence of a single crack in the biscuit did not appear to promote any greater dispersion in biscuit breakage characteristics but rather just acted to lower the mean breakage force.

4.5 Failure of Cracked Biscuits (Theoretical)

The validity of the failure criterion expressed by equation 8 was examined. Failure by fracture occurs when the calculated stress intensity factor, K_I equals the critical stress intensity factor (fracture toughness), K_{IC} of the biscuit. Because the magnitude of breakage forces for each crack is distributed (as quantified by the standard deviation in table 3) and the fracture toughness of the material itself varies (estimated mean value of 18 $kPam^{0.5}$ with standard deviation of 3 $kPam^{0.5}$), the level of agreement must be quantified statistically. From the experimental analysis presented in table 3, the cracked biscuits where failure was by fracture rather than crack propagation were identified. Table 4 summarises the results for these biscuits giving the crack identifier, the magnitudes of the relative depth, w/t and relative length, 2a/t, the maximum perpendicular stress at the crack (obtained from the mean value of breakage force in each case and using equation 6) and the corresponding stress intensity factor. Generally the theoretical predictions agree very well with the experimental findings with the average stress intensity factor for each crack type being close to the mean level of fracture toughness (18 $kPam^{0.5}$). The only exceptions are the three crack types E, J and P. The reason for the discrepancy for crack E is the inability of the Rice & Levy method to calculate the correct magnitude of the stress intensity factor for very short cracks. For crack types J and P, where the calculated stress intensity factor is considerably less than the fracture toughness the reason for the poor agreement is unknown but could reflect a statistical outlier effect. To assess the failure criterion more rigorously, the data is displayed graphically in figure 10. The stress intensity factor for each crack type is shown with error bars corresponding to ±1 standard deviation. Additionally the fracture toughness (critical stress intensity factor) is indicated by a solid line with the broken line representing its ± 1 standard deviation limits. Differences between the means of the stress intensity factor for each crack type and the mean critical stress intensity factor are quite small compared to the variability in K_I within each crack type (apart from types E, J and P). Applying the F statistic from ANOVA, demonstrated that the validity of the failure model (equation 8) could be accepted at the 5 % confidence level.

For all biscuits containing cracks, the mode of failure (fracture versus overloading) can be predicted by two loading ratios; the SIF ratio (K_I/K_{IC}) for the former and the failure stress ratio (σ_{max}/σ_f) for the latter. Whichever ratio is closer to 1, should determine the failure response; crack propagation for the former and overloading for the latter. This is the case for most of the crack types with failure by overloading occurring when the stress ratio is high and the stress intensity ratio relatively low while failure by crack propagation occurs for the reverse condition. Figure 11 gives a scatter plot of the two failure criteria for each crack type. Biscuits that failed by crack propagation are indicated with square markers and those by overloading with triangular markers. There is good demarcation between the failure mechanisms with biscuits that failed by overloading lying at the lower, right quadrant and biscuits that failed by crack propagation at the upper, left quadrant. Because the stress ratio lies with quite tight limits of 0.7 and 1.2 while the SIF ratio varies more widely (between 0.2 and 1.2,), the influence of the stress ratio, while present, is more difficult to discern. Finally regarding the critical crack size analysis of Section 2.4, inputting the data for our work gives a magnitude for the critical crack depth of 0.61 mm. In other words any long crack passing through the central zone with radius r_0' (3.28 mm) that is deeper than 0.61 mm should result in failure by fracture. This is confirmed by the experimental data of this work.

5. CONCLUSIONS

This work primarily has explored the force needed to break sound and cracked biscuits. It also measured the breakage pattern (number and size of fragment pieces). In particular, the structural behaviour of circular biscuits supported around the circumference and loaded by a central concentrated force has been examined. For a biscuit without defects, breakage occurred when biscuit stress reached or exceeded the failure stress. For a biscuit with defects such as checks or cracks, breakage occurred as above or alternatively when the critical stress intensity factor was reached. For the latter case, the breakage force was considerably reduced showing that cracks or checks considerably weaken the strength and integrity of the biscuit. Furthermore, a stress intensity factor model to quantify the effect of a crack on biscuit response has been proposed and verified. The effect of a crack on biscuit strength is dependent on crack depth, length, orientation and location on the biscuit surface. Shallow, short, radial cracks near the biscuit centre are more injurious to its integrity than deep, long cracks out near the biscuit circumference. Variability in biscuit properties, principally the tensile strength and critical stress intensity factor, complicate the issue and explain the scatter in the data. Biscuit breakage behaviour is closely connected to the quality parameter of texture. The results are relevant to understanding the maintenance of biscuit integrity through the post-manufacture, supply, distribution and transport chain that the biscuit endures prior to sale.

REFERENCES

Ahmad, S.S., Morgan, M.T. & Okos, M.R. (2001). Effect of microwave on the drying, checking and mechanical strength of baked biscuits. *Journal of Food Engineering*, 50, 63-75.

ASTM, (2008). ASTME1820, *Standard test method for measurement of fracture toughness*, ASTM International, West Conshocken, PA, USA.

Benham, P.P.; Crawford, R.J.; Armstrong, C.G. (1996). *Mechanics of Engineering Materials*. 2nd. Edition. Prentice Hall, New York, USA.

Consolmagno, G.J.; Britt, D.T. (1998). The density and porosity of meteorites from the Vatican collection. *Meteoritics & Planetary Science*, 33, 1231-1241.

Dunn, J.A.; Bailey, C.H. (1928). Factors influencing checking in biscuits. *Cereal Chemistry*, 5, 395-430.

Frisullo, P.; Conte, A.; Del Nobile, M.A. (2010). A novel approach to study biscuits and breadsticks using x-ray computed tomography. *Journal of Food Science*, 75(6): E353-E358.

Guessasma, S, Chaunier, L, Della Valle, G. & Lourdin, D. (2011). Mechanical modelling of cereal solid foods, *Trends in Food Science & Technology*, 22, 142 – 153.

Haghighi, K.; Segerlind, L.J. (1988). Failure of biomaterials subjected to temperature and moisture gradients using the finite element method. Parts I and II. *Transactions of the ASAE*, 31, 930-937, 938-946.

Kawai, K.; Toh, M.; Hagura, Y. (2014). Effect of sugar composition on the water sorption and softening properties of cookie. *Food Chemistry*, 145, 772-776.

Kawas, M.L.; Moreira, R.G. (2001). Characterization of product quality attributes of tortilla chips during the frying process. *Journal of Food Engineering*, 47, 97-107.

Kim, E.H-J.; Corrigan, V.K.; Wilson, A.J.; Waters, I.R.; Hedderly, D.I.; Morgestern, M.P. (2012). Fundamental fracture properties associated with sensory hardness of brittle solid foods. *Journal of Texture Studies*, 43, 49-62.

Legullion, D. & Piat, R. (2007). Fracture of porous materials – Influence of pore size, *Engineering Fracture Mechanics*, doi:10.1016/j.engfracmech.2006.12.002

Lim, K.S. & and Barigou, M. (2004). X-ray micro-computed tomography of cellular food products, *Food Research International*, 37, 1001 – 1012.

Mamat, H.; Hill, S.E. (2012). Effect of fat types on the structural and textural properties of dough and semi-sweet biscuit. *Journal of Food Science and Technology*, (Online First™ on 29 April 2012. doi:10.1007/s13197-012-0708-x).

Manley, D. (2000). *Technology of biscuits, crackers and cookies*. 3rd edn. Woodhead Publishing Limited, Cambridge.

Okpala, C.O.; Okoli, E.C. (2013). Optimization of composite flours biscuits by mixture response surface methodology. *Food Science and Technology International*, 19(4), 343-350.

Pareyt, B.; Talhaoui, F.; Kerchofs, G.; Brijs, K.; Goesaert, H.; Wevers, M.; Delcour, J.A. (2009). The role of sugar and fat in sugar-snap cookies: structural and textural properties. *Journal of Food Engineering*, 90: 400-408.

Ramakrishnan N. & Arunachalam, V.S. (1990). Effective elastic moduli of porous solids, *Journal of Material Science*, 25, 3930-3937.

Rice, J.R.; Levy, N. (1972). The part-through surface crack in an elastic plate. *Journal of Applied Mechanics*, 39(1), 185-194.

Rojo, F.J. & Vincent, J. F. V. (2008). Fracture properties of potato crisps, International *Journal of Food Science & Technology*, 43, 752-760.

Saleem, Q. (2005). Mechanical and fracture properties for predicting cracking in semi-sweet biscuits. *International Journal of Food Science and Technology*, 40, 361-367.

Sudha, M.L.; Vetrimani, R.; Leelavathi, K. (2007). Influence of fibre from different cereals on the rheological characteristics of wheat flour dough and on biscuit quality. *Food Chemistry*, 100, 1365-1370.

Van Vliet, T., (2014). *Rheology and Fracture Mechanics of Foods*, CRC Press, Taylor & Francis, Boca Raton, FL, USA.

Vujić, L.; Cepo, D.V.; Dragojevic, I.V. (2014). Impact of dietetic tea biscuit formulation on starch digestibility and selected nutritional and sensory characteristics. *LWT - Food Science and Technology*, 1-7.

Yang, B. & Shiva, S. (2011). Crack growth with a part-through process zone in thin plates, *International Journal of Fracture*, 168, 145-158.

Young, W.C. (2001). *Roark's formulas for stress & strain*, 7th Edition, McGraw-Hill, New York, USA.

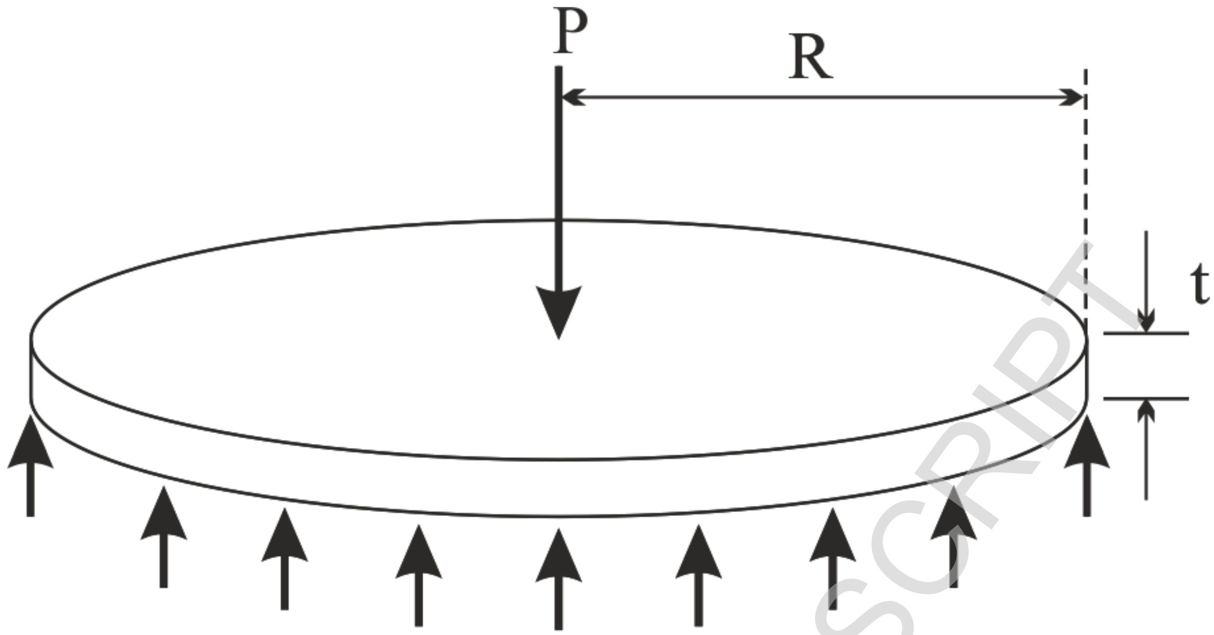

Figure 1 Biscuit loading geometry

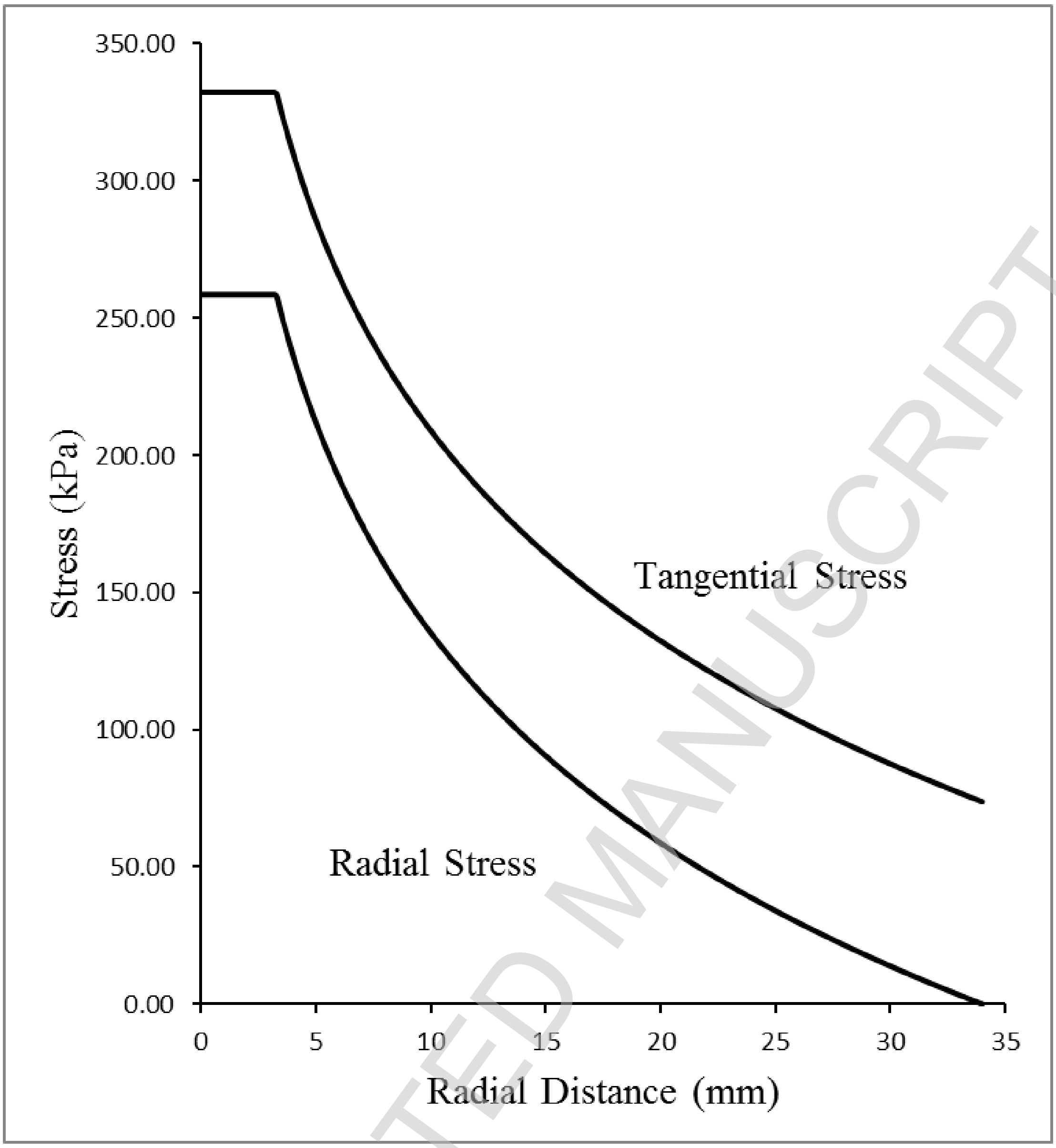

Figure 2: Typical variation of tangential and radial stress with radial distance (R = 34 mm, t = 7.2 mm, r_0 = 3 mm, υ = 0.2, P = 10 N).

.

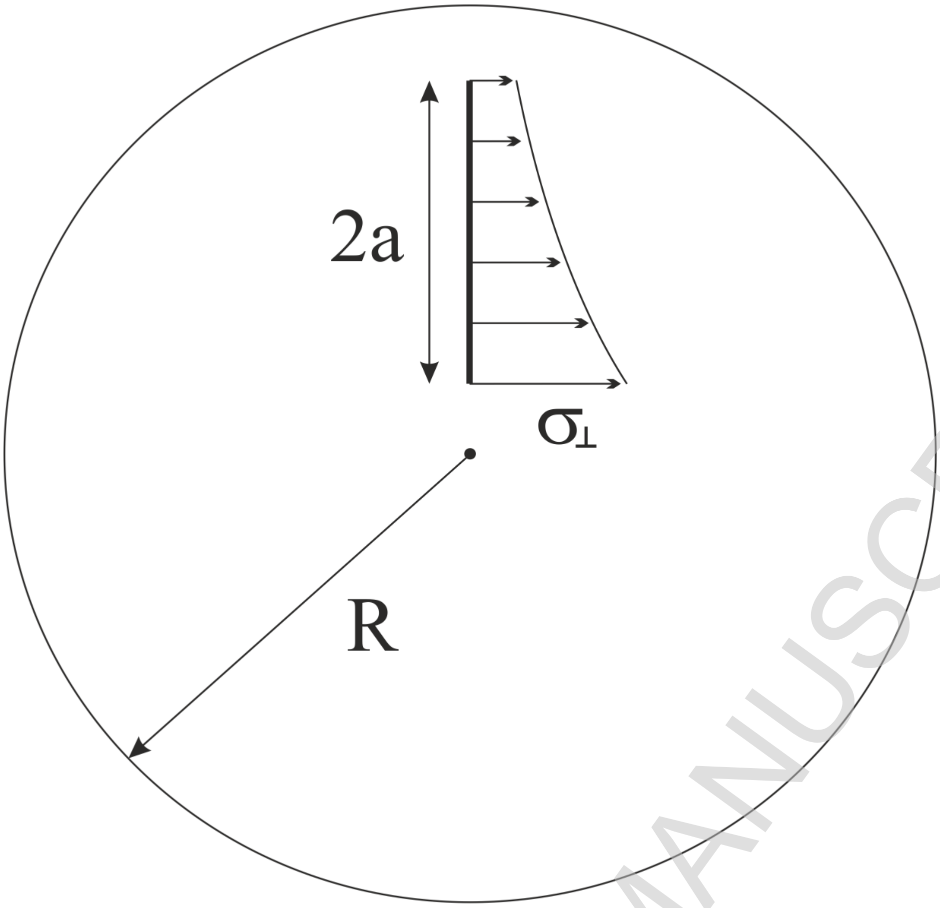

Figure 3a Perpendicular stress along a radial line

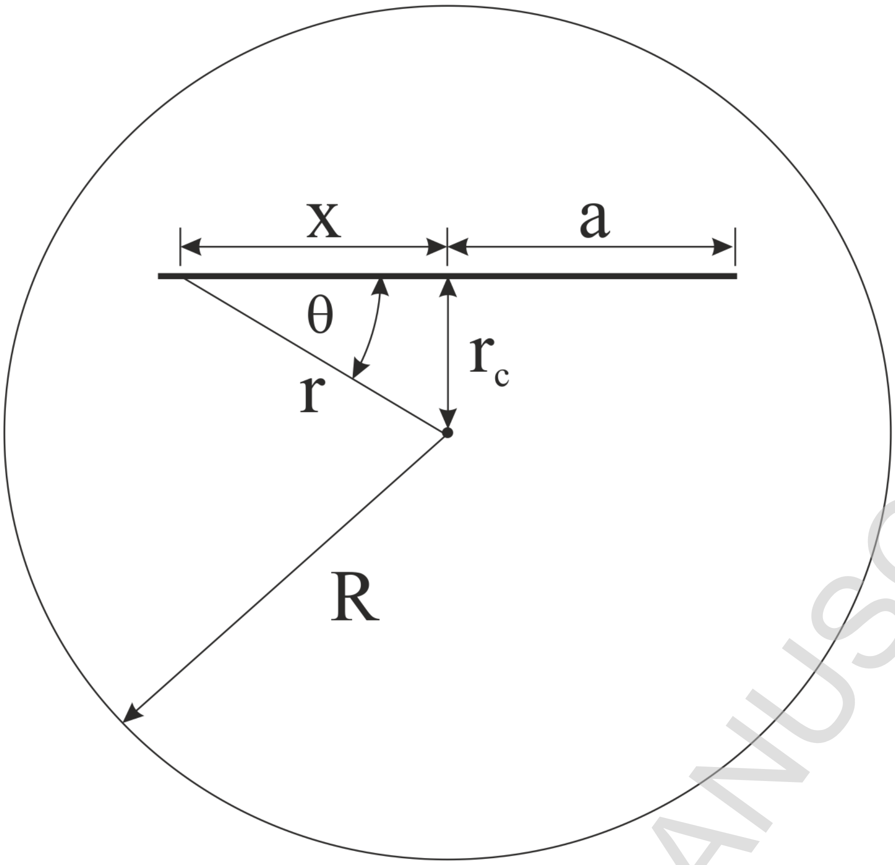

Figure 3b Tangential line geometry

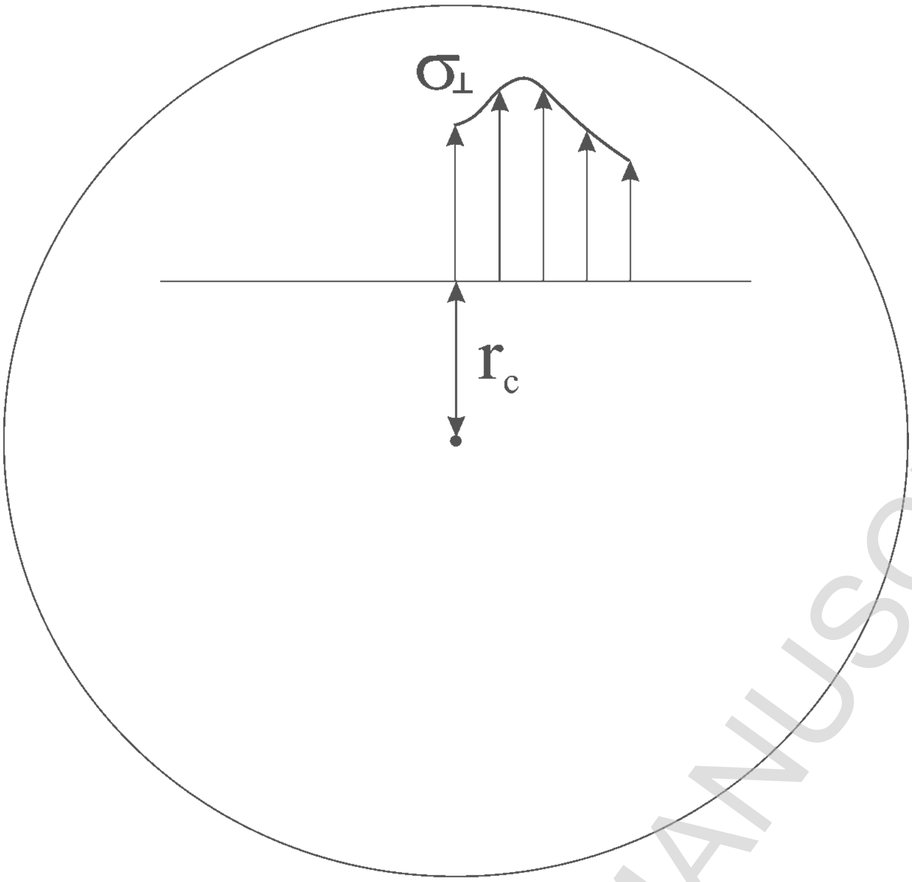

Figure 3c Perpendicular stress along a tangential line

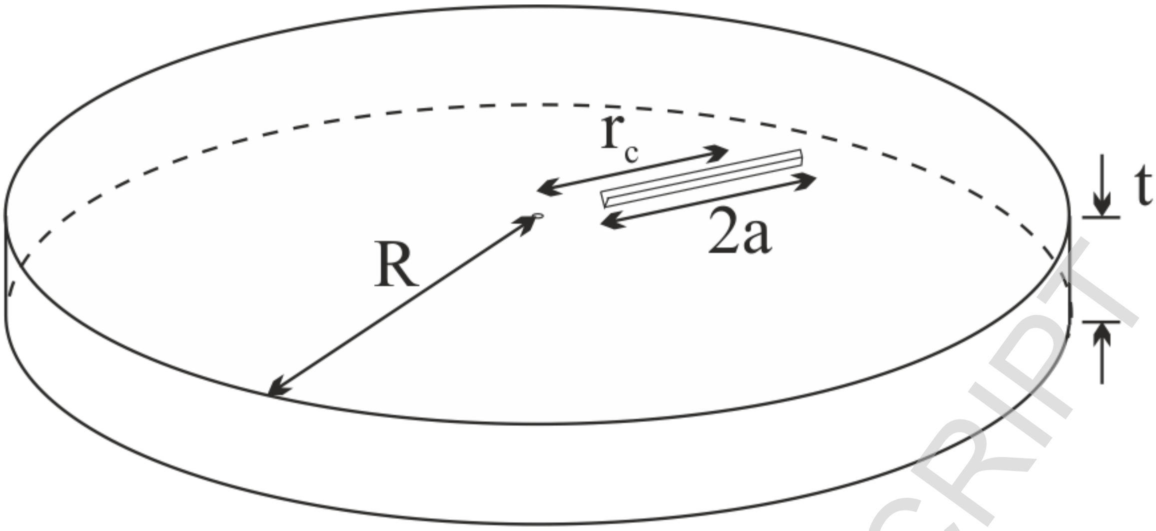

Figure 4 Crack geometrical parameters

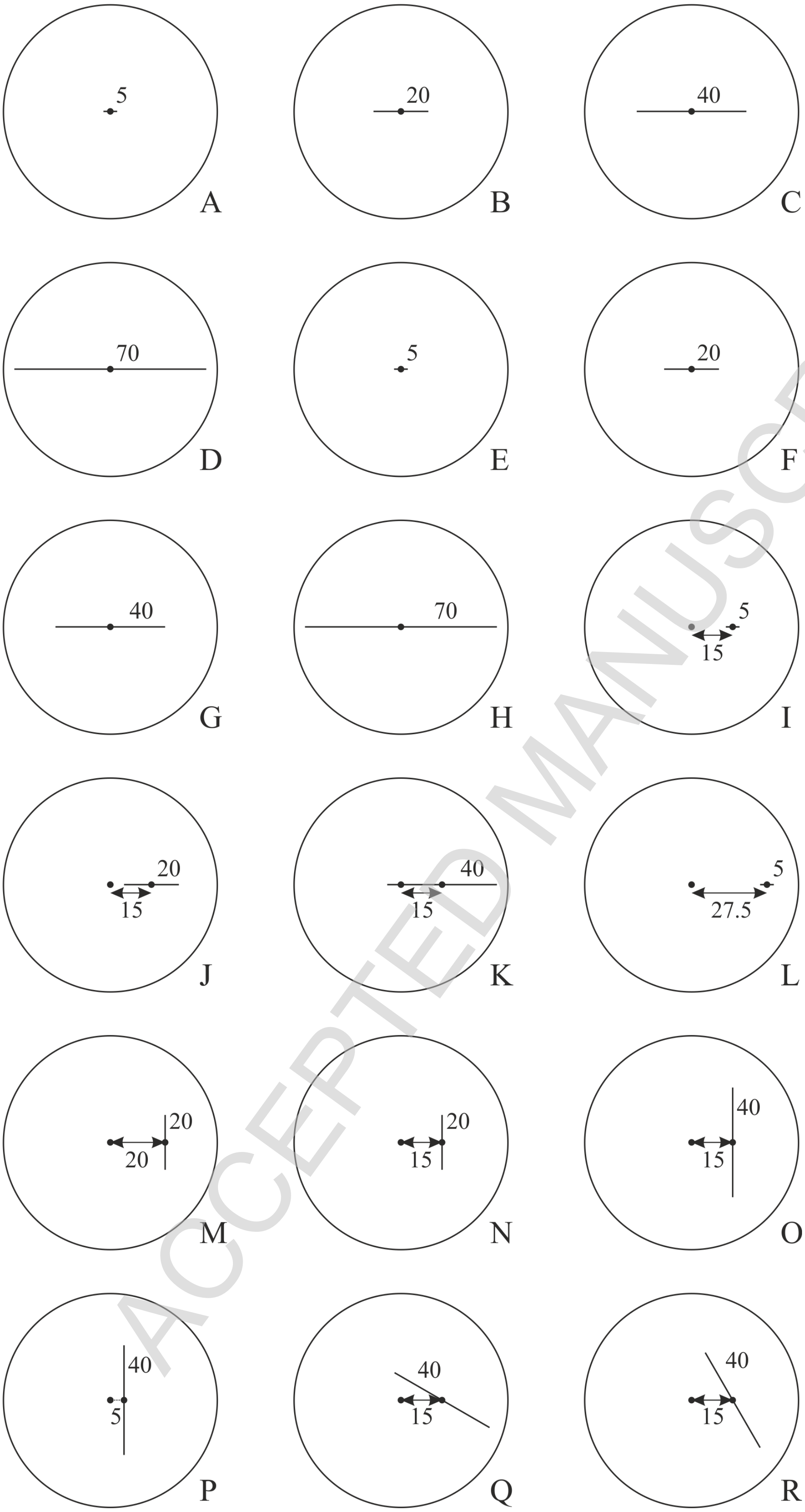

Figure 5: Crack geometries

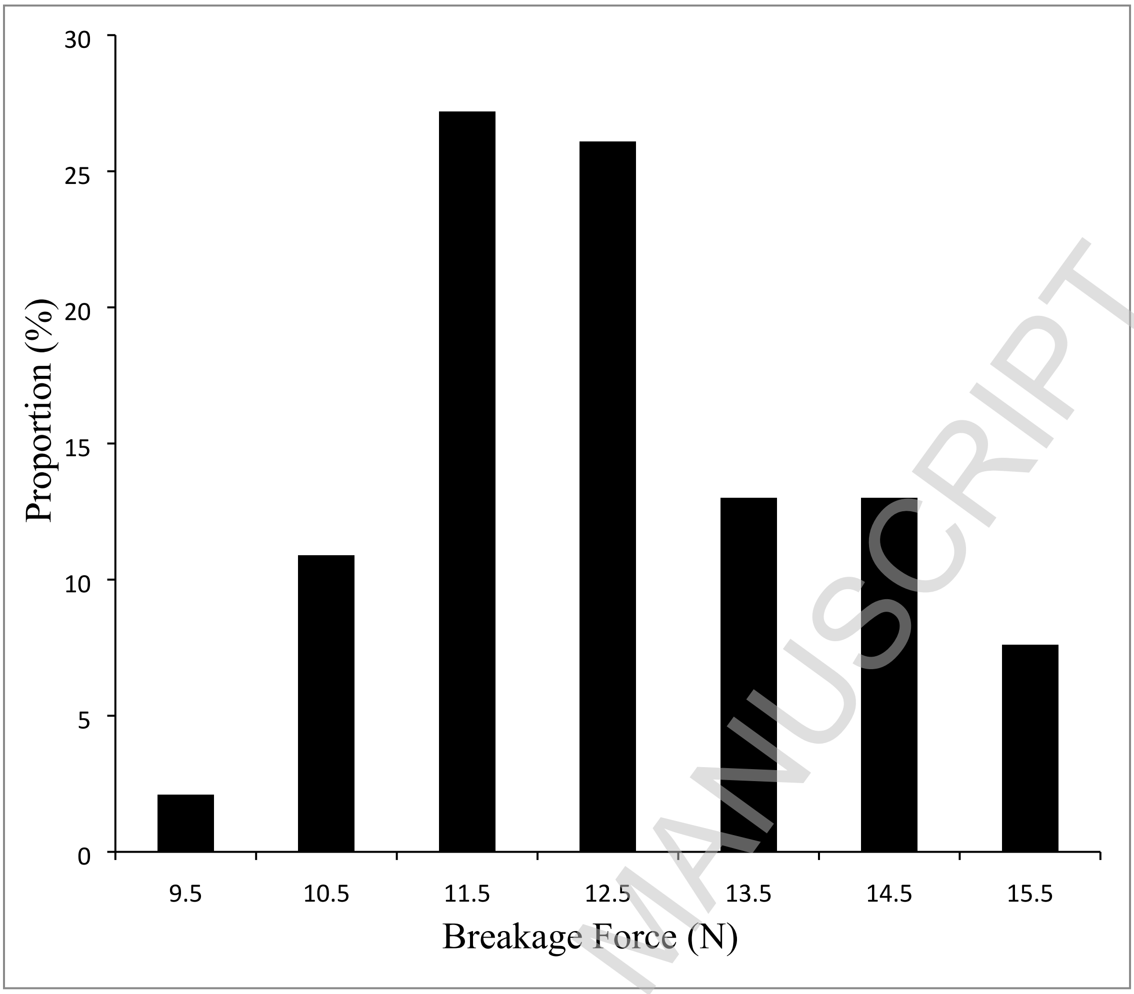

Figure 6 Distribution of the breakage force for biscuits without checks

Figure 7 Breakage modes for biscuits without checks (Two radial cracks, Three radial cracks, Four radial cracks)

ACCEPTED MANUSCRIPT

Figure 8 Checked biscuits

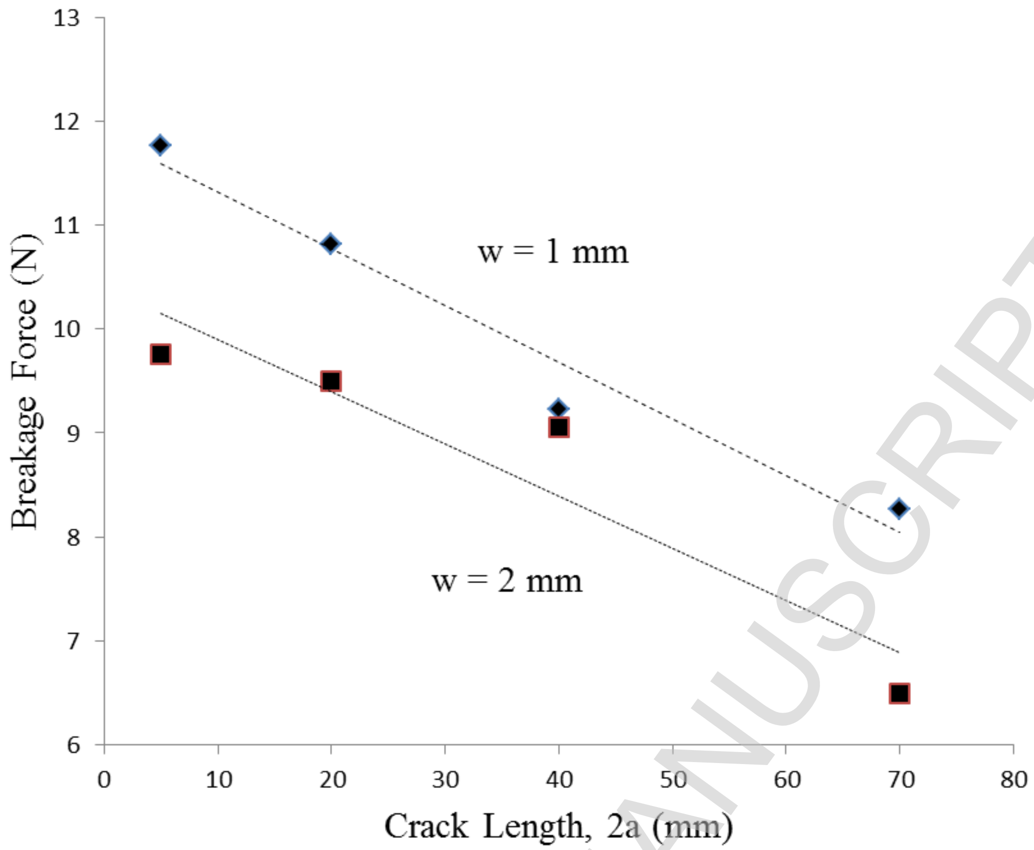

Figure 9 Breakage force versus crack length for two crack depths

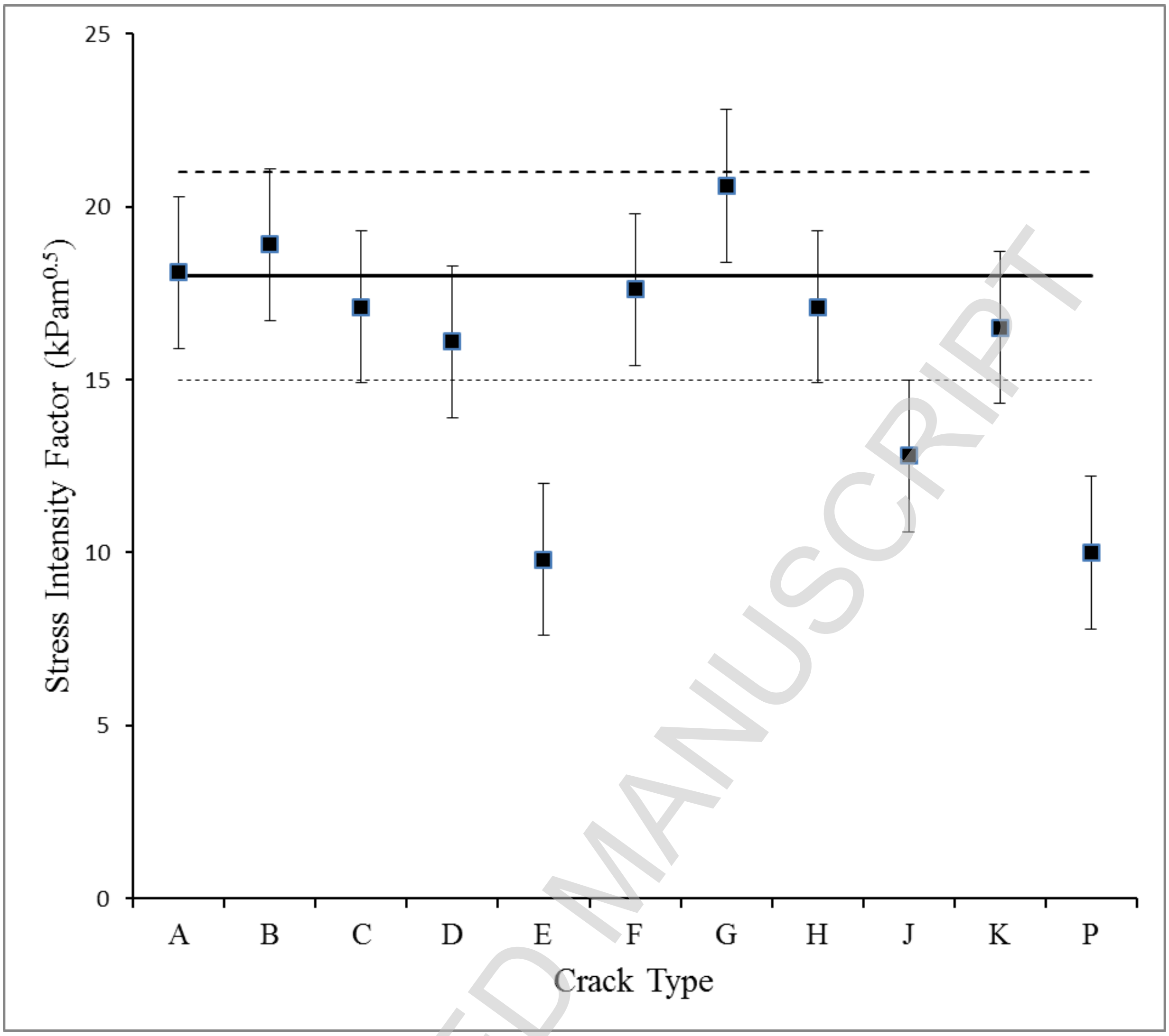

Figure 10: Failure analysis of cracked biscuits

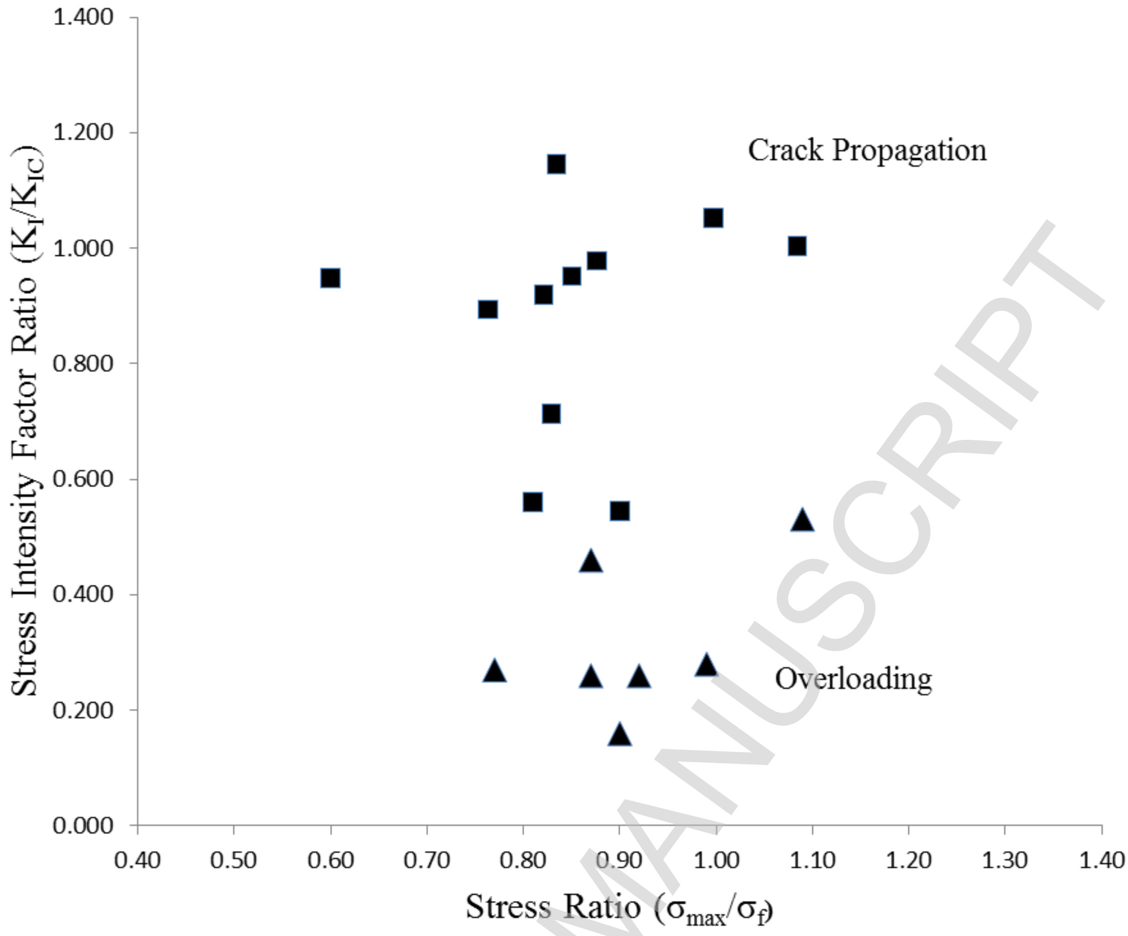

Figure 11 Analysis of biscuit failure modes

Figure List

Relative crack depth (w/t)	c_1 Parameter	c_2 Parameter
0.14	0.0755	0.7795
0.28	0.2004	0.4006
0.46	0.2105	0.0869

Table 1: Values of the fracture model parameters c_1 and c_2 (extracted from Rice & Levy, 1972)

Crack Identifier	Crack Orientation	Mid-Point Location	Crack Length	Crack Depth
		mm	mm	mm
A	Radial	0	5	1
B	Radial	0	20	1
C	Radial	0	40	1
D	Radial	0	70	1
E	Radial	0	5	2
F	Radial	0	20	2
G	Radial	0	40	2
H	Radial	0	70	2
I	Radial	15	5	1
J	Radial	15	20	1
K	Radial	15	40	1
L	Radial	27.5	5	1
M	Tangential	20	20	1
N	Tangential	15	20	1
O	Tangential	15	40	1
P	Tangential	5	40	1
Q	30° Angle	15	40	1
R	60° Angle	15	40	1

Table 2: Crack geometrical parameters

Crack Identifier	Crack Type	Breakage Force	Failure Mode
		N	
Uncracked Biscuit		12.5 ± 1.2	Overload
A	Radial	11.76 ± 1.15	Crack Prop.
B	Radial	10.82 ± 1.39	Crack Prop.
C	Radial	9.23 ± 1.41	Crack Prop.
D	Radial	8.27 ± 1.35	Crack Prop.
E	Radial	9.76 ± 0.33	Crack Prop.
F	Radial	9.5 ± 2.68	Crack Prop.
G	Radial	9.06 ± 1.13	Crack Prop.
H	Radial	6.5 ± 0.82	Crack Prop.
I	Radial	11.82 ± 1.05	Overload
J	Radial	9.0 ± 1.78	Crack Prop.
K	Radial	8.89 ± 1.33	Crack Prop.
L	Radial	9.92 ± 1.07	Overload
M	Tangential	9.72 ± 0.7	Overload
N	Tangential	10.7 ± 0.54	Overload
O	Tangential	9.36 ± 1.05	Overload
P	Tangential	8.79 ± 0.93	Crack Prop.
Q	30°	9.36 ± 1.05	Overload
R	60°	8.34 ± 0.75	Overload

Table 3: Failure loads and mechanisms for cracks

Crack Identifier	w/t	2a/t	$\sigma_{\perp\ max}$	K_I
			kPa	$kPam^{0.5}$
A	0.139	0.694	412	18.1
B	0.139	2.778	379	18.9
C	0.139	5.556	323	17.1
D	0.139	9.722	290	16.1
E	0.278	0.694	342	9.8
F	0.278	2.778	333	17.6
G	0.278	5.556	317	20.6
H	0.278	9.722	228	17.1
J	0.139	2.778	257	12.8
K	0.139	5.556	312	16.5
P	0.139	5.556	188.5	10.0

Table 4: Cracked biscuit failure analysis

List of Tables